Nuclear Instruments and Methods in Physics Research B xxx (2015) xxx–xxx

Contents lists available at ScienceDirect

Nuclear Instruments and Methods in Physics Research B

journal homepage: www.elsevier.com/locate/nimb

Monte-Carlo modeling of excitation of the electron subsystem of ZnO and MgO in tracks of swift heavy ions

R.A. Voronkov [a], R.A. Rymzhanov [b], N.A. Medvedev [c], A.E. Volkov [b,d,e,*]

[a] National Research Nuclear University MEPhI, Kashirskoe highway 31, 115409 Moscow, Russia
[b] FLNR, JINR, Joliot-Curie 6, 141980 Dubna, Russia
[c] CFEL at DESY, Notkestr. 85, 22607 Hamburg, Germany
[d] NRC Kurchatov Institute, Kurchatov Sq. 1, 123182 Moscow, Russia
[e] LPI of the Russian Academy of Sciences, Leninskij prospekt, 53, 119991 Moscow, Russia

ARTICLE INFO

Article history:
Received 16 May 2015
Received in revised form 13 July 2015
Accepted 16 July 2015
Available online xxxx

Keywords:
TREKIS
Swift-heavy ion
Electron kinetics
Ballistic spreading

ABSTRACT

Monte Carlo code TREKIS is applied to trace kinetics of excitation of the electron subsystem of ZnO and MgO after an impact of a swift heavy ion (SHI). The event-by-event simulations describe excitation of the electron subsystems by a penetrating SHI, spatial spreading of generated electrons and secondary electron cascades. Application of the complex dielectric function (CDF) formalism for calculation of the cross sections of charged particle interaction with a solid target allows to consider collective response of the target to perturbation, which arises from the spatial and temporal correlations in the target electrons ensemble. The method of CDF reconstruction from the experimental optical data is applied. Electron inelastic mean free paths calculated within the CDF formalism are in very good agreement with NIST database. SHI energy losses agree well with those from SRIM and CasP codes. The radial distributions of valence holes, core holes and delocalized electrons as well as their energy densities in SHI tracks are calculated. The analysis of these distributions is presented.

1. Introduction

A swift heavy ion (SHI, $M > 10\ m_p$, $E > 1$ MeV/a.m.u.) penetrating in a solid loses the main part of its energy (>95%) on excitation of the electronic subsystem [1–3]. Further relaxation of the excess energy of the electron subsystem may cause significant structure transformations in nanometric proximity of the SHI trajectory, which makes SHIs as a possible tool for nanostructuring of materials. High level of the energy deposition into the electron subsystem of a target along an SHI track (5–30 keV/nm) as well as extremely small spatial and temporal scales leads to unusual kinetic pathways of a material excitation [4]. A complete picture of these pathways is yet unknown, but the possible effects including ballistic spreading of electrons, nonequilibrium electronic and atomic kinetics, ultrafast electron-lattice coupling resulting in energy and momentum exchange, are studied in this work.

In this paper Monte-Carlo (MC) code TREKIS [5] is applied to describe excitation of the electronic subsystem of MgO and ZnO irradiated with Bi 700 MeV ion. ZnO and MgO are extremely resistant to radiation damage induced by fusion fragments and fast ions decelerated in the electronic stopping regime. This makes these materials perspective for nuclear and space technologies (e.g. MgO was proposed for inert matrixes of the composite nuclear fuel [6]). Understanding of the nature of this resistance is important for the both: (a) development of new radiation-resistant materials, and (b) development of adequate models of the kinetics of excitation and relaxation of dielectrics originated from extreme excitation of their electronic subsystems in the vicinity of the SHI trajectories as well as in spots of femtosecond laser pulses.

The complex dielectric function (CDF) formalism [7–9] is applied to obtain the cross sections of interaction of charged particles with matter. This formalism takes automatically into account effects of collective response of the electronic and ionic subsystems of materials to excitation caused by a penetrating particle. The calculated cross sections of SHI and electrons scatterings are then incorporated into the Monte Carlo model, which simulates ionization of a target by an incident ion, electron cascades, and Auger decays of holes in deep atomic shells.

We calculated the temporal dependencies of the radial distributions of electrons and holes densities and their energy densities around the trajectory of a Bi ion (700 MeV) in MgO and ZnO. These distributions can be used as initial condition for models describing electron-lattice energy exchange and subsequent

* Corresponding author at: NRC Kurchatov Institute, Kurchatov Sq. 1, 123182 Moscow, Russia.

http://dx.doi.org/10.1016/j.nimb.2015.07.088
0168-583X/

possible structure transformations in the vicinity of the SHI trajectories in these materials [10–12].

2. Model

2.1. Complex dielectric function formalism

The cross section of interaction of a charged projectile with a system of spatially and dynamically correlated scattering centers can be obtained within the first Born approximation as a product of the cross section of scattering on an individual charged center and the "charge–charge" dynamic structure factor [8] of the system. According to the fluctuation–dissipation theorem, this dynamic structure factor of a solid can be expressed in terms of the inverse imaginary part of CDF, $\varepsilon(\omega,\boldsymbol{q})$ (the loss function) [7,9,13], resulting in the following form of the double differential cross section:

$$\frac{d^2\sigma}{d\omega dq} = \frac{2(Z_e e)^2}{\pi\hbar^2 \upsilon^2}\frac{1}{q}\mathrm{Im}\left(\frac{-1}{\varepsilon(\omega,\boldsymbol{q})}\right) \quad (1)$$

here, σ is the cross section of a particle scattering (the double differential one over the transferred energy $\hbar\omega$ and momentum $\hbar\boldsymbol{q}$, $\hbar$ is the Plank constant); Z_e is the equilibrium charge of a particle penetrating through the electronic system as a function of the particle velocity (for an incident electron $Z_e = 1$, for an SHI the dependence of Z_e on the ion velocity is calculated with the Barkas formula [14,15]); e is the electron charge; υ is the velocity of the incident particle.

Richie and Howie [7] proposed an algorithm allowing to obtain the loss function using experimental data on photoabsorption. The method is based on fitting of the CDF reconstructed from experimental data with a set of the Drude-type CDF for artificial oscillators:

$$\mathrm{Im}\left[\frac{-1}{\varepsilon(\omega, q=0)}\right] = \sum_i \frac{A_i\gamma_i\hbar\omega}{\left(\hbar^2\omega^2 - E_{0i}^2\right)^2 + (\gamma_i\hbar\omega)^2} \quad (2)$$

here, E_{0i} is the characteristic energy of an oscillator i, A_i is the fraction of electrons with energy E_{0i}, and γ_i is the i-th energy damping coefficient, the summation is running through all the oscillators. The procedure of finding these coefficients is described in Refs. [7,9].

The quality of the obtained fitting functions can be checked by fulfilling the sum-rules [8–10]. When $\hbar\omega_{\max} \to \infty$, according to the *ps*-sum-rule (limiting form of the Kramers–Kronig integral), the value $P_{\mathrm{eff}} = 2/\pi \int_0^{\omega_{\max}} \mathrm{Im}[\varepsilon(\omega, q=0)^{-1}]d\omega/\omega$ must tend to 1, and the *f*-sum-rule, which is the oscillator strength that describes the total number Z of electrons per atom, states that the value $Z_{\mathrm{eff}} = 2/(\pi\Omega_p^2)\int_0^{\omega_{\max}} \mathrm{Im}[\varepsilon(\omega, q=0)^{-1}]\omega d\omega$ must approach the total number of electrons per molecule of a target. Here, $\Omega_p^2 = (4\pi n_m e^2/m_e)^{1/2}$ is the plasma frequency, n_m is the density of molecules of a solid under consideration, m_e is the free electron mass. The obtained coefficients for MgO and ZnO for scattering on optical phonons, valence band and on the deep shells as well as the fulfillment of the sum rules is presented in Tables 1 and 2.

The above described formalism allows us to calculate the partial cross-sections of an electron scattering by collision with the valence band and deeper shell electrons (inelastic processes) as well as on optical phonons of a solid (elastic scattering) i.e. the CDF formalism automatically takes into account the collective response of a target, e.g. plasmons and optical part of lattice collective modes [16,17].

In present approach we neglect the collisions between an SHI and target atoms due to low probabilities of such processes.

Table 1
The coefficients of the CDF fitted in the form of oscillator functions, Eq. (2), which provide a good agreement with the experimental optical data for MgO [32,33]: the total *f*-sum rule gives 20.14 (only 0.7% deviation from the total number of electrons $Z_{\mathrm{eff}} = 20$).

Name	E_{0i}	A_i	γ_i	*f*-Sum (number of electrons)
Phonon peak	0.09	0.0029	0.0035	
Valence band	40	370	60	8.0528 (8)
	5	−0.7	3	
	23.5	5	1	
	11.7	0.8	0.5	
	6.9	−0.5	1	
	15	13	3	
	20.3	17	2	
	22.2	64	2	
	25	60	3	
	30	65	15	
	89	510	145	
L-shell of Mg	72	35	12	8.0613 (8)
	94	80	40	
K-shell of O	538	212	400	2.0103 (2)
K-shell of Mg	1300	205	1100	2.0135 (2)
Total				20.14 (20)

Table 2
The coefficients of the CDF fitted in the form of oscillator functions, Eq. (2), which provide a good agreement with the experimental optical data for ZnO [33–35]: the total *f*-sum rule gives 38.11 (only 0.29% deviation from the total number of electrons $Z_{\mathrm{eff}} = 38$).

Name	E_{0i}	A_i	γ_i	*f*-Sum (number of electrons)
Phonon peak	0.073	0.0007	0.003	
Valence band with a part of M-shell	9	1.5	2	23.955 (24)
	20	75	4	
	23	46	4	
	26	30	4	
	32	70	12	
	42	64	15	
	60	1100	112	
M1-shell of Zn	185	137	150	2.066 (2)
K-shell of O	400	260	300	2.056 (2)
L-shell of Zn	1000	655	815	7.968 (8)
K-shell of Zn	8000	200	7400	2.065 (2)
Total				38.11 (38)

2.2. Monte Carlo model

The calculated cross sections are then introduced into the MC code TREKIS [5] which has been already successfully applied for describing electron kinetics in an SHI track in various solids (LiF, Y_2O_3, SiO_2, Al_2O_3, Si, Ge, Al [15,18,19]). Asymptotic trajectory Monte Carlo method using the Poisson distribution for the free-flight distance [20,21] and the mean free path of a projectile scattering is applied to simulate propagation of a charged particle (an SHI and electrons) and its interactions with the electron subsystem. During penetration of an SHI or an electron through a solid, the target electrons are considered as uniformly distributed particles occupying either the atomic energy levels [22] or the states in the valence band according to the density of states (DOS) of the materials [23]. In the framework of the independent particle model, it is assumed that excitation of an electron does not affect the others during the collision. Taking into account large velocities of projectiles, we assume these electrons as point-like particles at

Please cite this article in press as: R.A. Voronkov et al., Monte-Carlo modeling of excitation of the electron subsystem of ZnO and MgO in tracks of swift heavy ions, Nucl. Instr. Meth. B (2015), http://dx.doi.org/10.1016/j.nimb.2015.07.088

fixed positions during their energy and momentum exchange with an SHI. The energy transfer ΔE_e to electrons is calculated from the differential cross section, Eq. (1).

The holes in deep atomic shells are relaxing quickly via Auger decays with characteristic times taken from Ref. [24], and all are eventually popping up into the valence band. The decay times of holes are sampled with the Poisson distribution. The shells, participating in the Auger decay, are chosen randomly. The emission of the Auger electron is assumed to be uniform into the solid angle. All these electron and hole cascades are simulated event by event. In the present work we neglect valence holes propagation out of the ion trajectory. Thus, no effects of ambipolar diffusion or other kinds of interaction between electrons and holes are included.

TREKIS simulates penetration of an SHI which incidents perpendicularly to the surface of a layer of ~10–100 nm thickness with periodic boundary conditions (cylinder geometry). An ion performs initial ionization of a target creating the first generation of free electrons. Due to the heavy mass of a projectile ($M_{\text{ion}} \gg m_e$) and its negligible scattering on target atoms for energies considered here, the SHI trajectory is assumed to be a straight line.

Finally, the MC procedure is iterated for 10^3 times to get a trustworthy statistics. That gives the temporal dependencies of the radial distributions of electrons and holes in different atomic shells and their energy densities in an SHI track. The calculations were performed up to 1000 fs after the ion impact. These distributions can be used as input parameters (initial conditions and/or source terms) in further modeling of the lattice heating, material modifications and phase transitions caused by an SHI passage [10,11,25,26].

3. Results and discussion

Fig. 1 presents the calculated mean free path of electrons compared to the data from the National Institute of Standards and Technology (NIST) database [27,28]. A very good agreement of presented data with NIST predicative formulae (Fig. 1a) and data from other authors (Fig. 1b) confirms the validity of the calculated cross sections of electron inelastic scattering in these solids.

Calculated ion energy loss of Bi in MgO and ZnO compared to results of SRIM and CasP codes [29,30] are shown in Fig. 2. An overall good agreement between TREKIS and SRIM results confirms an applicability of the obtained fitting coefficients for the loss-function for modeling of SHIs impacts. Only a slight disagreement occurs for these results at low ion energies, which is expectedly caused by limits of validity of the model assumptions.

On the other hand, the energy losses in the region of the Bragg peak calculated by TREKIS and SRIM for MgO and ZnO differ about 1.2–1.5 times from those calculated within CasP code. This indicates the necessity of experimental verification of the losses for these oxides.

Fig. 3 presents the temporal dependencies of the radial distributions of generated free electrons and their energy densities. The figure demonstrates ballistic propagation of the front outwards from the track center. This front is formed by spreading through

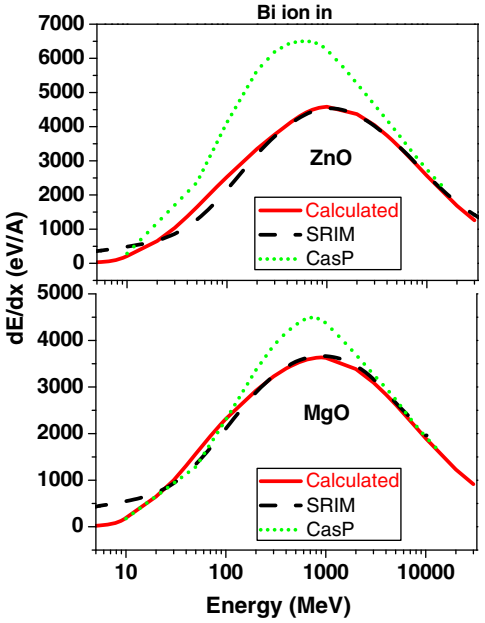

Fig. 2. The calculated energy losses of Bi ion in ZnO (a) and in MgO (b) as functions of the ion energy, compared to the SRIM and CasP data [28,29].

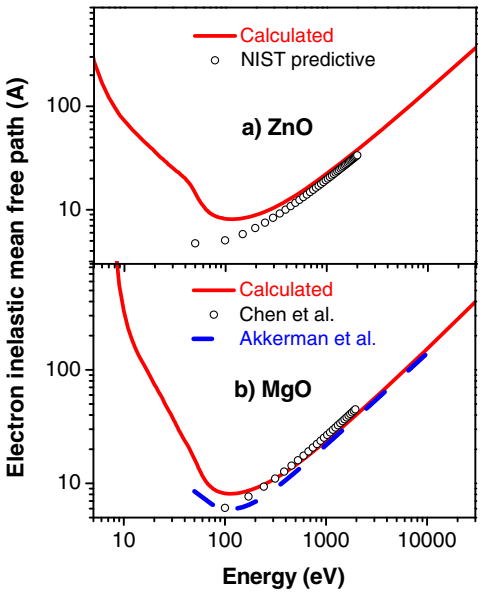

Fig. 1. The calculated electron inelastic mean free paths in solid ZnO (a) and in MgO (b) targets, compared with the predictive formulae [28] and the data from the other authors available in NIST database.

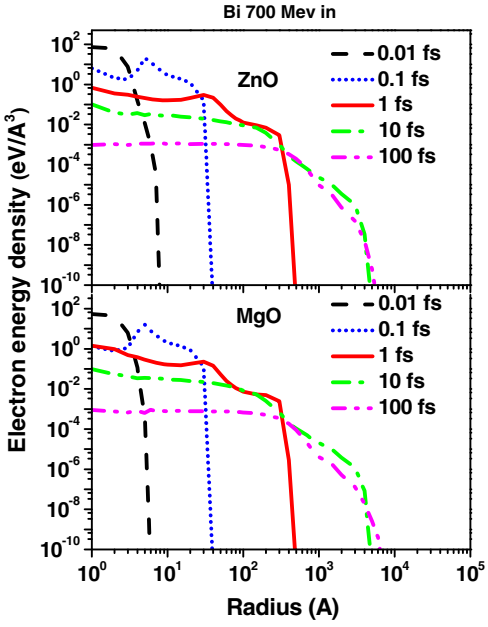

Fig. 3. The calculated electron radial energy distributions in ZnO (a) and MgO (b) around the trajectory of Bi (700 MeV) ion at different times after the ion passage.

Please cite this article in press as: R.A. Voronkov et al., Monte-Carlo modeling of excitation of the electron subsystem of ZnO and MgO in tracks of swift heavy ions, Nucl. Instr. Meth. B (2015), http://dx.doi.org/10.1016/j.nimb.2015.07.088

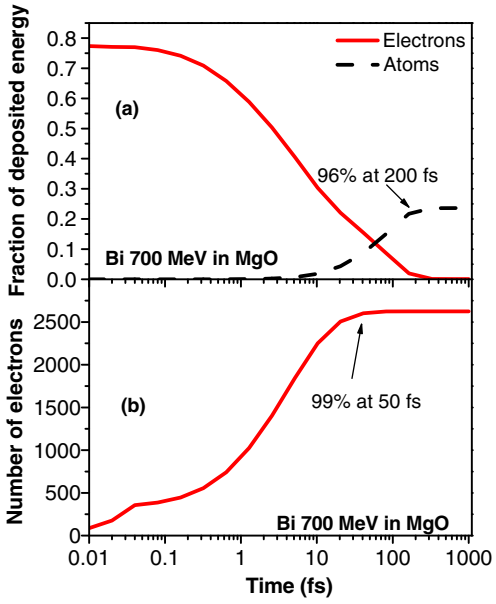

Fig. 4. The calculated fraction of energy deposited into MgO electrons (solid line) and atoms (dash line) by Bi 700 MeV ion (a) and the total number of emitted electrons in an Bi ion track in MgO as the function of time after SHI impact (b).

an unexcited medium of fast primary δ-electrons produced directly by the SHI. The peak in the spatial energy distribution following after the front of primary electrons is a result of a generation of a large amount of secondary electrons with the energy around the plasmon frequency. Emergence of the diffusive behavior of the secondary electrons is indicated by smearing out of this peak occurring at times of a few tens of femtoseconds.

Fig. 4a demonstrates that electron-lattice coupling lasts up to ~200 fs when the greatest part (>96%) of the appearing excess lattice energy have been already transferred by electrons. Taking into account the characteristic times of phonons oscillations (~100 fs) this means that electron–phonon coupling model can be applied only on the latest stage of electron-lattice energy and momentum exchange in an ion track (see also [4,26,31]).

Fig. 4b shows the temporal dependence of the total number of generated electrons in an SHI track in MgO after passage of Bi 700 MeV ion. One can see that the greatest part of generated electrons (about 99%) around Bi track has been already produced at times ~50 fs. It's interesting to mention that the fractions of energy deposited into MgO by penetrating Bi ion are the same for electrons and atoms at 50 fs (Fig. 4a). Thus, by the end of ionization cascades, a large amount of energy is already transferred to the atomic system of this material.

4. Conclusions

This paper presents MC code TREKIS applied to simulations of the kinetics of the electron ensemble in Bi ion (700 MeV) tracks in MgO and ZnO. The applied cross sections, the mean free paths of electrons as well as the ion inelastic energy loses were calculated using complex dielectric function formalism. The calculated data demonstrate a very good agreement with NIST database and SRIM and CasP codes.

The radial distributions of the concentrations and energy densities of electrons at different times after the SHI passage are calculated. These distributions can serve as initial conditions for models describing electron-lattice energy and momentum exchange in SHI tracks in MgO and ZnO.

Time dependent calculations show ballistic propagation of front of excitation in the electron subsystem. Also they show the peak following after this front which is a result of a generation of large amount of secondary electrons with the energy around the plasmon frequency. Smearing out of this peak at times above 10 fs indicates the beginning of diffusive behavior of propagation of the excitation.

The transient total number of emitted electrons and fractions of the energy deposited by an SHI are presented. These dependences demonstrate the characteristic timescales of processes in an SHI track.

Acknowledgements

The results were obtained using computational resources of MCC NRC "Kurchatov Institute" (http://computing.kiae.ru/) and CICC LIT JINR (http://lit.jinr.ru/). Partial financial support from grants 13-02-12020, 15-02-02875, 15-58-15002 of Russian Foundation for Basic Research is acknowledged by A.E. Volkov.

References

[1] F. Aumayr, S. Facsko, A.S. El-Said, C. Trautmann, M. Schleberger, J. Phys.: Condens. Matter 23 (2011) 393001.
[2] F.F. Komarov, Phys. Usp. 46 (2003) 1253–1282.
[3] A.M. Stoneham, N. Itoh, Appl. Surf. Sci. 168 (2000) 186–193.
[4] A.E. Volkov, V.A. Borodin, Nucl. Instr. Meth. Phys. Res. B 146 (1998) 137–141.
[5] N.A. Medvedev, R.A. Rymzhanov, A.E. Volkov, J. Phys. D Appl. Phys. (2015) (accepted).
[6] A. Imaura, N. Touran, R.C. Ewing, J. Nucl. Mater. 389 (2009) 341–350.
[7] R.H. Ritchie, A. Howie, Philos. Mag. 36 (1977) 463–481.
[8] L. Van Hove, Phys. Rev. 95 (1954) 249–262.
[9] A. Akkerman, T. Boutboul, A. Breskin, R. Chechik, A. Gibrekhterman, Y. Lifshitz, Phys. Status Solidi B 198 (1996) 769–784.
[10] O. Osmani, N. Medvedev, M. Schleberger, B. Rethfeld, Phys. Rev. B 84 (2011) 214105.
[11] S.A. Gorbunov, N.A. Medvedev, P.N. Terekhin, A.E. Volkov, Nucl. Instr. Meth. Phys. Res. B 354 (2015) 220–225.
[12] D.M. Duffy, S.L. Daraszewicz, J. Mulroue, Nucl. Instr. Meth. Phys. Res. B Beam Interact. Mater. Atoms 277 (2012) 21–27.
[13] J.-C. Kuhr, H.-J. Fitting, J. Electron Spectros. Relat. Phenomena 105 (1999) 257–273.
[14] W.H. Barkas, Nuclear Research Emulsions, New York, 1963.
[15] N.A. Medvedev, R.A. Rymzhanov, A.E. Volkov, Nucl. Instr. Meth. Phys. Res. B 315 (2013) 85–89.
[16] N.W. Ashcroft, N.D. Mermin, Solid States Physics, Rinehart and Winston Holt, New York, 1976.
[17] D. Pines, Elementary Excitations in Solids, W.A. Benjamin Inc., New-York, Amsterdam, 1963.
[18] R.A. Rymzhanov, N.A. Medvedev, A.E. Volkov, Nucl. Instr. Meth. Phys. Res. B. 326 (2014) 238–242.
[19] R.A. Rymzhanov, N.A. Medvedev, A.E. Volkov, Phys. Status Solidi B 252 (2015) 159–164.
[20] B. Gervais, S. Bouffard, Nucl. Instr. Meth. Phys. Res. B 88 (1994) 355–364.
[21] A. Akkerman, M. Murat, J. Barak, Nucl. Instr. Meth. Phys. Res. B 269 (2011) 1630–1633.
[22] J.A. Bearden, A.F. Burr, Rev. Mod. Phys. 39 (1967) 125–142.
[23] M. Huang, W. Ching, Phys. Rev. B: Condens. Matter 54 (1996) 5299–5308.
[24] O. Keski-Rahkonen, M.O. Krause, At. Data Nucl. Data Tables 14 (1974) 139–146.
[25] M.C. Ridgway, T. Bierschenk, R. Giulian, B. Afra, M.D. Rodriguez, L.L. Araujo, et al., Phys. Rev. Lett. 110 (2013) 245502.
[26] M. Toulemonde, C. Dufour, E. Paumier, Phys. Rev. B 46 (1992) 14362–14369.
[27] C.J. Powell, A. Jablonski, J. Phys. Chem. Ref. Data 28 (1999) 19.
[28] C.J. Powell, A. Jablonsky, 2014 <http://www.nist.gov/srd/nist71.cfm>.
[29] J.P. Ziegler, U. Biersack, J.F. Littmark, The Stopping and Range of Ions in Solids, Pergamon Press, New York, 1985.
[30] P.L. Grande, G. Schiwietz, Nucl. Instr. Meth. Phys. Res. B 267 (2009) 859–863.
[31] S.a. Gorbunov, N.a. Medvedev, P.N. Terekhin, a.E. Volkov, Nucl. Instr. Meth. Phys. Res. B Beam Interact. Mater. Atoms 354 (2015) 220–225.
[32] E.D. Palik, Handbook of Optical Constants of Solids, Academic Press, San Diego, 1985.
[33] B.L. Henke, E.M. Gullikson, J.C. Davis, At. Data Nucl. Data Tables 54 (1993) 181–342.
[34] S. Adachi, The Handbook on Optical Constants of Semiconductors: In Tables and Figures, World Scientific Publishing Company, 2012.
[35] P. Ooi, S. Lee, S. Ng, Z. Hassan, H.A. Hassan, J. Mater. Sci. Technol. 27 (2011) 465–470.

Please cite this article in press as: R.A. Voronkov et al., Monte-Carlo modeling of excitation of the electron subsystem of ZnO and MgO in tracks of swift heavy ions, Nucl. Instr. Meth. B (2015), http://dx.doi.org/10.1016/j.nimb.2015.07.088